Eur. Phys. J. B **7**, 67–77 (1999)

THE EUROPEAN PHYSICAL JOURNAL B

EDP Sciences
© Società Italiana di Fisica
Springer-Verlag 1999

Unified quantum mechanical picture for confined spinons in dimerized and frustrated spin S = 1/2 chains

G.S. Uhrig[1,a], F. Schönfeld[1], M. Laukamp[2], and E. Dagotto[2]

[1] Institut für Theoretische Physik, Universität zu Köln, Zülpicher Straße 77, 50937 Köln, Germany
[2] National High Magnetic Field Laboratory and Department of Physics, Florida State University, Tallahassee, Florida 32306, USA

Received: 8 May 1998 / Revised and Accepted: 12 August 1998

Abstract. A quantum mechanical picture is presented to describe the behavior of confined spinons in a variety of $S = 1/2$ chains. The confinement is due to dimerization and frustration and it manifests itself as a nonlinear potential $V(x) \propto |x|^b$, centered at chain ends ($b \leq 1$) or produced by modulation kinks ($b > 1$). The calculation extends to weak or zero frustration some previous ideas valid for spinons in strongly frustrated spin chains. The local magnetization patterns of the confined spinons are calculated. A (minimum) enhancement of the local moments of about 11/3 over a single $S = 1/2$ is found. Estimates for excitation energies and binding lengths are obtained.

PACS. 64.70.Kb Solid-solid transitions – 75.10.Jm Quantized spin models – 75.50.Ee Antiferromagnetics

1 Introduction

Dimerized and frustrated spin chains have attracted considerable interest in recent years. This is due to the recent emergence of a variety of experimental quasi-one-dimensional systems containing localized electrons that can be described by spin chains. Among these systems there is a sizable number which are gapful due to dimerization in their low temperature phase, such as $CuGeO_3$ [1], α'–NaV_2O_5 [2], $(VO)_2P_2O_7$ [3], $Cu(NO_3)_2 \cdot 2.5H_2O$ [4], $CuWO_4$ [5], and $Cu_2(C_2H_{12}N_2)_2Cl_4$ [6]. The first two dimerize as a consequence of the coupling to the lattice degrees of freedom, whereas the other compounds are intrinsically dimerized, *i.e.* the dimerization does not depend on temperature. The effect of doping on these substances represents an interesting issue, in particular since it pertains also to defects such as missing spins, broken chains and chains of finite length.

As a general rule, defects in low-dimensional antiferromagnetic spin systems which can be described by a RVB-type ground state [7] involve $S = 1/2$ states in their vicinity [8]. The appearance of a certain impurity spin at the edges of spin chains can also be discussed in the framework of a nonlinear σ model for general spin S [9]. We restrict ourselves to $S = 1/2$, weakly dimerized spin chains. The basic idea there is that without the defect each spin has a partner with which a singlet is formed. If the defect removes one of the partners, the other becomes a free $S = 1/2$ spin which we will henceforth call spinon to distinguish it from the other singlet forming spins. We understand that this spinon comprises also some dressing of the bare $S = 1/2$ spin, *i.e.* it is not localized at just one site. Since the singlet pairing is not static in the RVB-picture the spinon is able to move some distance away from the defect. In a critical, gapless system it will be delocalized. This delocalization, however, disappears as soon as the couplings are modulated.

It is the purpose of this work to elucidate in which way an explicit dimerization acts as a confining potential for the spinon motion leading to its localization. The generic Hamiltonian reads

$$H = J \sum_i \left((1 + (-\delta)^i) \mathbf{S}_i \cdot \mathbf{S}_{i+1} + \alpha \mathbf{S}_i \cdot \mathbf{S}_{i+2} \right) \quad (1)$$

where δ parametrizes the dimerization and α the relative frustration by next-nearest neighbor coupling. Previous works, *e.g.* [10–13], viewed dimerization already as confining potential. We understand that there is no confinement without dimerization ($\delta = 0$). Here we will develop a quantum mechanical picture that treats the cases of small and large frustration on equal footing. Although this picture is not exact in all details, nevertheless it is able to reproduce the main features of the problem on a semi-quantitative level. The physical quantities considered here are binding energies and local magnetizations. In addition, it will be shown that the confinement depends on the degree of frustration and it will be sublinear in the region of low frustration.

For the sake of concreteness, the case of a chain end is illustrated in Figure 1. Dimerization localizes spin singlets mostly at the strong bonds. If in a dimerized chain

[a] e-mail: gu@thp.uni-koeln.de

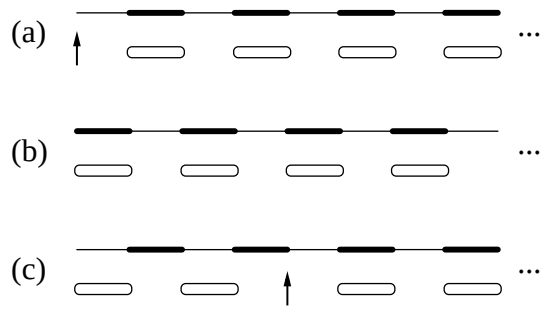

Fig. 1. Three possible configurations at chain ends. The thick (thin) solid lines stand for strong (weak) bonds; the open eyelets stand for singlets, the arrow for an unpaired spin. (a) weak bond at the chain end corresponds to a free spin; (b) strong bond at the chain end corresponds to no free spin; (c) configuration after two hops of the free spin from (a). Note the misaligned first two singlets at the strong bonds.

one spin is missing its singlet partner is freed. If the missing spin had a weak bond to the left (assuming without loss of generality horizontal chains) and a strong bond to the right, the free spin situation corresponds to the one in Figure 1a. The configuration in Figure 1b is then the reflected configuration found on the left of the missing spin. If the missing spin had a strong bond to the left and a weak bond to the right, the free spin situation is found to the left of the missing spin. The configuration in Figure 1a is then a reflected image whereas the configuration in Figure 1b is found to the right of the missing spin. Figure 1c illustrates the situation after two hops of the free spin away from its origin in (a). The crucial point is that the singlets to the left of the spin in Figure 1c are no longer at the strong bonds. This implies an energy loss which can be viewed as an attractive potential which ties the free spin to its origin. Besides chain ends also solitonic modulations, such as kink defects, will be considered in this paper. They can also be viewed as spinon traps with confining potentials.

The article is organized in the following way. In the next section, the short-range RVB spinon states that determine the main part of the correlations will be introduced. Subsequently, the forms of the kinetic and the potential energies which govern the spinon dynamics will be discussed, *i.e.* the Schrödinger equation of the problem will be setup. In the fourth and the fifth sections the quantitative results will be discussed and compared against computational calculations for chain ends and for kink-modulated chains, respectively. A summary will conclude the article.

2 States: Norm and magnetization

Let us denote by $|i\rangle$ an up-spinon at site $2i+1$; the other spins are all paired to nearest-neigbor singlets. In this convention, the state in Figure 1a is denoted by $|0\rangle$ and the state in Figure 1c is denoted by $|2\rangle$. These states are not orthogonal but their overlap [7,14,15] is given by

$$\langle i|j\rangle = \left(-\frac{1}{2}\right)^{|i-j|}. \tag{2}$$

This overlap arises from a Néel type sequence of up-spins and down-spins between the two spinons. Let us consider a state

$$|v\rangle = \sum_{i=0}^{\infty} a_i (-1)^i |i\rangle \tag{3}$$

for which we aim to obtain a continuum description. This means that we assume that for the low energy behavior it is sufficient to treat a_i as a slowly varying function of i. Note that we introduced the factor $(-1)^i$ to focus on the energetically low-lying states. This can be seen most easily for $\alpha = 1/2$ [14–16]. In order to define a normalized wave function $\psi(x)$ let us calculate the norm of $|v\rangle$

$$\begin{aligned}\langle v|v\rangle &= \sum_{i,j} a_i^* a_j \left(\frac{1}{2}\right)^{|i-j|} \\ &\approx \sum_i |a_i|^2 \left(-1 + 2\sum_{j=0}^{\infty} 2^{-j}\right) \\ &= 3\sum_i |a_i|^2. \end{aligned} \tag{4}$$

The approximate step is valid if a_i varies in fact slowly with i. Equation (4) tells us that passing to a normalized continuous wave function $\psi(x)$ means $i \to x/2$ and $a_i \to \sqrt{2/3}\psi(x)$. The factor 2 introduced here enables the replacement of x by the actual site numbers at the end of the calculation.

Now we calculate the local magnetizations $m_l := \langle S_l^z \rangle$.

$$\langle v|S_l^z|v\rangle = \frac{(-1)^{l+1}}{2} \sum_{\substack{2i+1 \le l \le 2j+1 \text{ or} \\ 2j+1 \le l \le 2i+1}} a_i^* a_j \left(\frac{1}{2}\right)^{|i-j|}. \tag{5}$$

A contribution is found only if S_l^z is situated *between* the two spinons which equals one half of the overlap (2). For l odd one finds

$$\begin{aligned}\langle v|S_l^z|v\rangle &\approx |a_{(l-1)/2}|^2 \frac{1}{2}\left(-1 + 2\sum_{n,m=0}^{\infty}\left(\frac{1}{2}\right)^{n+m}\right) \\ &= \frac{7}{2}|a_{(l-1)/2}|^2 \\ &= \frac{7}{3}|\psi(l)|^2 \end{aligned} \tag{6}$$

where n and m stand for half the distance to site l on the left and on the right. We do not take the chain end into account, *i.e.* we ignore the fact that summation for small

l is truncated on the left. For even sites l one obtains

$$\begin{aligned}\langle v|S_l^z|v\rangle &\approx -\frac{1}{2}|a_{l/2}|^2 2\frac{1}{2}\sum_{n,m=0}^{\infty} 2^{-n-m}\\ &\approx -2|a_{l/2}|^2\\ &= -\frac{4}{3}|\psi(l)|^2. \end{aligned} \tag{7}$$

With the above calculation the local magnetizations have been linked to the probability of finding the spinon at a given site l. The sum $\sum_l m_l$ equals to one half as it has to be for a global $S = 1/2$ state. Note that to obtain this result one has to sum even and odd sites separately, and that l changes, thus, by two from site to site.

Summing the moduli $\sum_l |m_l|$ one gets immediately $(11/3)(1/2)$. This means that the antiferromagnetic correlations induce total local moments that correspond to the moments of $11/3 = 3.667$ independent spins $S = 1/2$. This enhancement factor of $11/3$ illustrates why even a low concentration of dopants may induce considerable antiferromagnetism in a compound [8,17,18]. Moreover, this enhancement is not due to criticality but it is already built-in in the short-range RVB state. The possible coexistence of dimerization and alternating local magnetization was nicely demonstrated by Fukuyama *et al.* by analysis of the corresponding phase hamiltonian [17]. Impurity-induced antiferromagnetism is already extensively investigated for spin ladders [19–24].

In the next paragraphs we will refine the calculation of the norm and the local magnetization by considering indeed a discrete wave function. We would like to remove the non-orthogonality of our basis states in order to be on safer ground for the subsequent reasoning. Moreover, certain boundary effects can be captured by this procedure.

By Gram-Schmidt orthogonalization we find the orthonormal basis

$$|w_0\rangle := |0\rangle \tag{8a}$$

$$|w_{i>0}\rangle := (-1)^i \frac{2}{\sqrt{3}}(|i\rangle + |i-1\rangle). \tag{8b}$$

The above definitions simplify any norm calculation. The magnetization calculation becomes a bit more tedious. For odd $l = 2j+1$ we have

$$\langle w_{j+1}|S^z_{2j+1}|w_{j+1}\rangle = -1/6 \tag{9a}$$

$$\langle w_j|S^z_{2j+1}|w_j\rangle = 1/2 \quad \text{for } j = 0 \tag{9b}$$

$$\langle w_j|S^z_{2j+1}|w_j\rangle = 1/3 \quad \text{for } j > 0 \tag{9c}$$

$$\langle w_j|S^z_{2j+1}|w_i\rangle = 2^{-1-j+i} \quad \text{for } j > i > 0 \tag{9d}$$

$$\langle w_j|S^z_{2j+1}|w_0\rangle = 2^{-j}/\sqrt{3} \tag{9e}$$

and the analogous formulae hold for $i \leftrightarrow j$. All other expectation values are zero. From the relations (9) one finds for a normalized state $|v\rangle = \sum_{i=0}^{\infty} b_i|w_i\rangle$

$$\langle v|S_1^z|v\rangle = \frac{1}{2}|b_0|^2 - \frac{1}{6}|b_1|^2 \tag{10a}$$

$$\begin{aligned}\langle v|S^z_{2j+1}|v\rangle = \frac{1}{3}|b_j|^2 - \frac{1}{6}|b_{j+1}|^2 +\\ + \text{Re } b_j^* 2^{-j}\left(\frac{2}{\sqrt{3}}b_0 + \sum_{i=1}^{j-1} b_i 2^i\right).\end{aligned} \tag{10b}$$

Repeating the same for even $l = 2j$ we arrive at

$$\langle w_j|S^z_{2j}|w_j\rangle = 1/3 \tag{11a}$$

$$\langle w_j|S^z_{2j}|w_i\rangle = -2^{-1-j+i} \text{ for } 0 < i < j \tag{11b}$$

$$\langle w_j|S^z_{2j}|w_0\rangle = -2^{-j}/\sqrt{3}. \tag{11c}$$

From equations (11) we obtain

$$\langle v|S^z_{2j}|v\rangle = \frac{1}{3}|b_j|^2 - \text{Re } b_j^* 2^{-j}\left(\frac{2}{\sqrt{3}}b_0 + \sum_{i=1}^{j-1} b_i 2^i\right). \tag{12}$$

Note that for $l \gg 0$ and slowly varying b_i one re-obtains, of course, the results equations (6, 7). This concludes the calculation of the local magnetizations.

3 Kinetic and potential energy

In this section we address the important issue of how the simple spinons introduced in the previous paragraph move and how they are attracted by the chain end. We will distinguish two regimes of frustration (i) $0.5 \geq \alpha > \alpha_c = 0.241$ [25,26] and (ii) $\alpha \leq \alpha_c$.

In regime (i) we know that the spinons have a finite mass and that they have a quadratic minimum in their dispersion [14–16]. Moreover, the strongly frustrated chains display spontaneous symmetry breaking of the translational symmetry, *i.e.* spontaneous dimerization occurs. The actual value of the gap (and the dimerization), however, is very small up to $\alpha = 0.35$ [27,28] (see also Fig. 3).

In regime (ii) the spinon dispersion is linear in the wave vector k [29]. Hence we assume $\omega(k) = v_S|k|$ where v_S is the spin wave velocity which is roughly given by

$$v_S = \frac{\pi}{2}(1 - 1.12\alpha) \tag{13}$$

according to references [29,30]. The multiplication by $|k|$ in reciprocal space can be visualized as the consecutive multiplications $k\,\text{sgn}(k)$. To multiply by k corresponds to $-i\partial/\partial x$ in real space, while a multiplication by $\text{sgn}(k)$ corresponds to the convolution with the principal value of $i/(\pi x)$. Then, $|k|$ in reciprocal space corresponds to the convolution

$$H_{kin}\psi(x) = -i\frac{\partial}{\partial x}\mathcal{P}\int_{-\infty}^{\infty}\frac{i}{\pi(x-y)}\psi(y)dy \tag{14a}$$

$$= -\frac{1}{\pi}\mathcal{P}\int_{-\infty}^{\infty}\frac{i}{(x-y)^2}\psi(y)dy. \tag{14b}$$

The symbol $\mathcal{P}$ stands for the principal value which has to be taken. If one has to discretize the singular operator H_{kin}, the most reliable approach to follow is to go back a few steps using $\omega(k) = v_S|\sin(ka)|/a$ in k-space and then transform this to real space yielding

$$H_{kin}\psi(r_i) = -\frac{1}{\pi}\sum_j \frac{4a\psi(r_j)}{4(r_i - r_j)^2 - 1} \tag{15}$$

where a is the lattice constant.

If we want to treat a chain end, a modification turns out to be necessary. Calculating with equation (14) the spinon wave function for an undimerized odd size chain one finds that the spinon is strongly repelled from the borders. This is similar to the problem of having a quantum mechanical particle in a finite box where the wave functions are sine-like with nodes at the wall positions. It is due to the fact that the kinetic energy cannot be fully satisfied close to a wall since hopping processes through the wall are not possible. However, analyzing the numerical results (see for instance the uniform susceptibility χ_i^u in Fig. 9b of Ref. [18]) one realizes that the probability of finding the spinon at a given site is approximately constant. We interprete here the uniform susceptibility χ_i^u as calculated by Laukamp *et al.* [18] as a measure for the probability to find the spinon. From this observation we conclude that the walls not only truncate the hopping processes but that they induce also another effect. To account for the fact that an approximately constant spinon wave function is the ground state wave function for the problem without dimerization we modify equation (14) to

$$H'_{kin}\psi(x) = -\frac{1}{\pi}\mathcal{P}\int_{-\infty}^{\infty}\frac{i}{(x-y)^2}\psi(y)dy - \frac{\psi(x)}{\pi x}\cdot \tag{16}$$

The effect of this modification is most easily understood by going back to equation (14a) and exchanging the sequence of differentiation and convolution. A constant wave function yields a δ-function due to the initial jump. The resulting term is compensated by the $1/x$ term in equation (16). We like to stress that the modification is motivated only phenomenologically. It would be desirable to have a more microscopic justification as well.

Equivalently, the discrete version of equation (16) reads

$$H'_{kin}\psi(r_i) = -\frac{1}{\pi}\sum_j \frac{4a\psi(r_j)}{4(r_i - r_j)^2 - 1} - \frac{2\psi(r_i)}{\pi(2r_i - 1)} \tag{17}$$

if the site counting starts with $i = 1$ at the border. Thus, for chain ends with small frustration we will use equation (16) as kinetic energy. For bulk problems we will use equation (14). The corresponding discrete versions are equations (17, 15), respectively.

Thus far, we have discussed only the kinetic energy. Considering now the potential energy we first consider regime (i) and in particular the Majumdar-Ghosh point $\alpha = 0.5$ for which the ground state is identical to the short-range RVB state. As noted previously, *e.g.* [10,11], the confining potential is a linear one in this regime. The potential due to the dimerization δH_D with

$$H_D = \sum_{j=1}^{\infty}(-1)^j \mathbf{S}_{2j-1}\cdot\mathbf{S}_{2j} \tag{18}$$

is given by

$$V(2i+1) = \delta\left(\langle i|H_D|i\rangle - \langle 1|H_D|1\rangle\right). \tag{19}$$

By inspecting Figures 1a and 1c we find that $V(2i+1)$ increases by $(3/2)J$ if the spinon hops once, since one singlet on the strong bonds is lost on the right side whereas one singlet is inserted on the weak bonds on the left side. Thus we have

$$V(2i+1) = \delta\frac{3}{2}Ji. \tag{20}$$

This allows us to propose the following Schrödinger equation for the motion of the spinon

$$E\psi(x) = -\frac{J}{2m}\frac{\partial^2}{\partial x^2}\psi(x) + \frac{3\delta J}{4}x\psi(x) \tag{21}$$

with the restriction $x \geq 0$. The value of m can be found from a variational investigation of a single spinon and is found to be approximately $m = (1 + 7/\sqrt{65})^{-1} \approx 0.535$ [14,15]. Rescaling equation (21) by $x = \xi y$ with

$$\xi = (3m\delta/2)^{-1/3} \tag{22}$$

(the site spacing is set to unity) yields

$$E\tilde{\psi}(y) = J\left(\frac{(3\delta/4)^2}{2m}\right)^{1/3}\left(-\frac{\partial^2}{\partial y^2}\tilde{\psi}(y) + y\tilde{\psi}(y)\right). \tag{23}$$

The linear differential equation (23) with the boundary condition $\tilde{\psi}(0) = 0$ is solved by shifted Airy functions [31]

$$0 = -\frac{\partial^2}{\partial y^2}\mathrm{Ai}(y) + y\mathrm{Ai}(y) \quad \Rightarrow \tag{24a}$$

$$-z_i\mathrm{Ai}(y + z_i) = -\frac{\partial^2}{\partial y^2}\mathrm{Ai}(y + z_i) + y\mathrm{Ai}(y + z_i) \tag{24b}$$

where the z_i are the zeros of $\mathrm{Ai}(y)$ which define by $e_i = -z_i$ the eigenenergies of the rescaled problem. The normalization is given by $\tilde{\psi}(y) = \mathrm{Ai}(y + z_i)/|\mathrm{Ai}'(y + z_i)|$. Summarizing, using equation (22) we have obtained

$$E_i = -z_i J\left(\frac{(3\delta/4)^2}{2m}\right)^{1/3} \tag{25a}$$

$$\psi(x) = \frac{\mathrm{Ai}(x/\xi + z_i)}{\sqrt{\xi}|\mathrm{Ai}'(y + z_i)|}. \tag{25b}$$

The form of the wave functions are given in Figure 2 where ξ is made equal to unity.

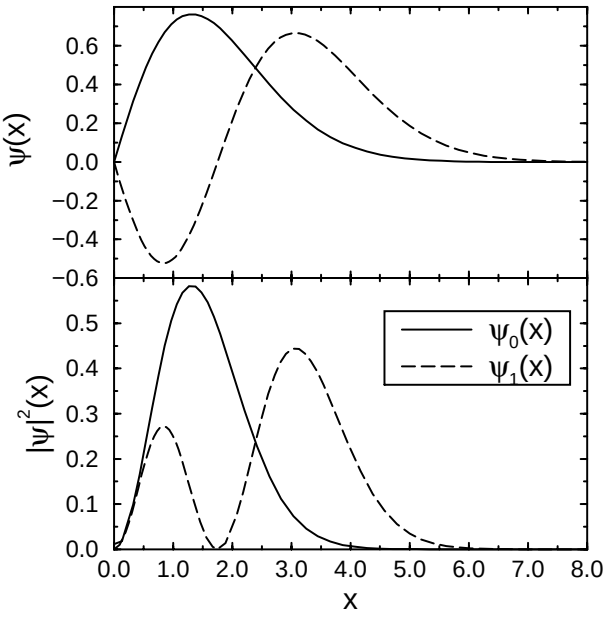

Fig. 2. Ground state and first excited state wave functions $\psi_0(x)$ and $\psi_1(x)$ using a linear potential $V(x) = x$ and a quadratic kinetic energy $H_{kin} = k^2$. The corresponding eigen energies are $e_0 = -z_0 = 2.338$ and $e_1 = -z_1 = 4.088$.

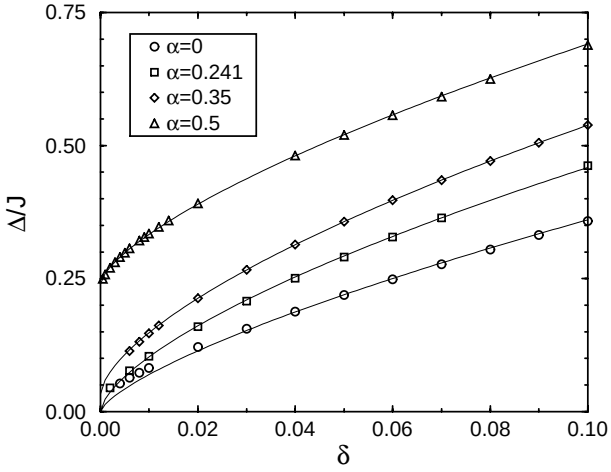

Fig. 3. Triplet gap as function of the dimerization δ for various values of the frustration α. Symbols are DMRG results; the solid lines are simple power law fits $\Delta \approx \Delta_0 + \Delta_1\delta^\nu$ with the parameters (α: Δ_0, Δ_1, ν) (0: 0, 1.57, 0.65); (0.241: 0, 2.05, 0.65); (0.35: 0.033, 2.216, 0.642); (0.5: 0.24, 2.183, 0.685). The absolute error is $10^{-4}J$ at most.

A linear potential together with a quadratic kinetic energy leads to energies proportional to $\delta^{2/3}$ if δ measures the potential strength. Such a behavior is actually observed in the dependence of the triplet gap $\Delta_{trip}(\delta)$ on the dimerization $\Delta_{trip}(\delta) - \Delta_{trip}(0) \propto \delta^{2/3}$, see Figure 3 and [28]. The corresponding calculation is almost equivalent to the above one since the triplet state can be viewed as two parallel spinons bound together by the same potential. Then, the coordinate x corresponds to the relative coordinate and the mass m has to be replaced by the relative mass $\mu = m/2$ since one has two kinetic energy contributions, see *e.g.* [11,13].

In the light of the success of a simple quantum mechanical picture for the case of large frustration we come back to case (ii) of subcritical frustration. Before entering the discussion we emphasize that without a gap there is *a priori* only a less good justification for a one-particle description since the length scale of the object carrying the $S = 1/2$ is the same as the spatial extent of the bound wave functions. Yet it is interesting to see that the simple model works well qualitatively and to a certain extent even quantitatively.

For subcritical frustration, we have two important pieces of information. The kinetic energy is linear in k, not quadratic. But the exponent of the (triplet) gap growth with dimerization is also 2/3 or close to it [27,28,32, 33] ($\Delta_{trip} \propto \delta^{2/3}$). To illustrate this point we show in Figure 3 gap data for four different values of the frustration. Power law fits with exponents close to 2/3 describe fairly well the gap growth in the subcritical and the supercritical frustration regime. The appropriate fit parameters, however, depend on the fit interval chosen. It is known that logarithmic corrections make it in general very difficult to observe the asymptotic behavior. Our estimations for the binding length (see below) provide additional information on how small the dimerization and how large the system have to be in order for the asymptotic behavior to be reached.

Thus far, we keep the information that the confining potential cannot be linear in the subcritical frustration regime. Revisiting the scaling that mapped equation (21) to the universal form equation (23) shows that the potential must grow as a square root $V(x) \propto \sqrt{x}$ in order to retain the exponent 2/3. This seems a very plausible conjecture which will be corroborated by a direct calculation of the potential.

In order to evaluate the potential energy between the chain end and the spinon we use ideas of Talstra *et al.* [34,35]. These authors have shown that a spinon state can be generated to 98% overlap by inserting a single spin in a spin chain which is otherwise in its ground state. If we take this idea over to our problem of a spinon and a chain end we may assume that the systems between the chain end and the spinon is in its undimerized ground state which is the ground state of a finite piece of chain with open boundary condition. We have to calculate the expectation value of the dimerization operator H_D (18) in this undimerized ground state in order to obtain an estimate for the potential. A small refinement is actually necessary since we are only interested in the expectation value of H_D with respect to the bulk limit. So we set $V(2i+1) = \langle H'_D\rangle_{2i}$ where the subscript $2i$ refers to the length of the finite piece of chain and

$$H'_D = \sum_{j=1}^{\infty}(-1)^j(\mathbf{S}_{2j-1}\cdot\mathbf{S}_{2j} - \langle\mathbf{S}_1\cdot\mathbf{S}_2\rangle_{bulk}). \qquad (26)$$

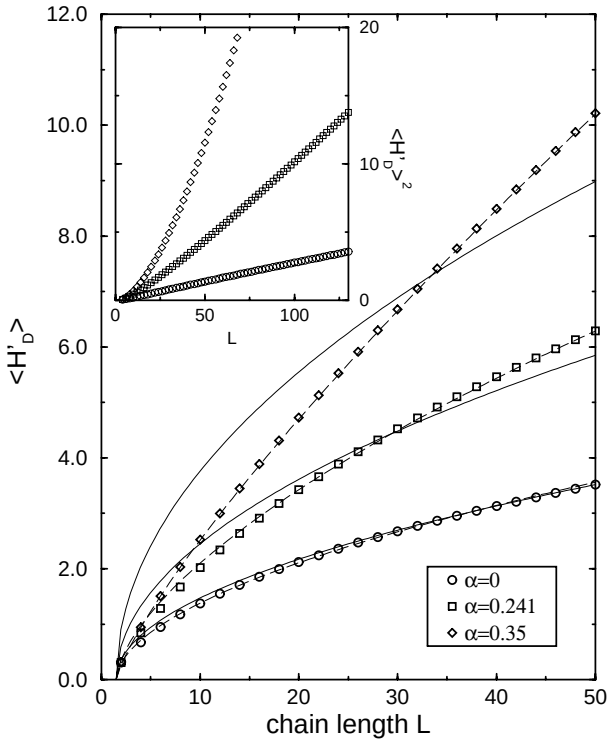

Fig. 4. Expectation value of H'_D as explained in the main text for three values of α. The solid lines are square root fits $\propto \sqrt{L-1.5}$ with the prefactors 0.505, 0.84, and 1.29 for $\alpha = 0$, 0.241, and 0.35. The offset 1.5 is chosen for the improvement of the fits. The dashed lines are power law fits $\propto (L-1.5)^{\beta}$ with the exponents and prefactors 0.544, 0.431 for $\alpha = 0$, 0.630, 0.545 for $\alpha = 0.241$, and 0.804, 0.450 for $\alpha = 0.35$. Inset: Square of the same data for longer chains.

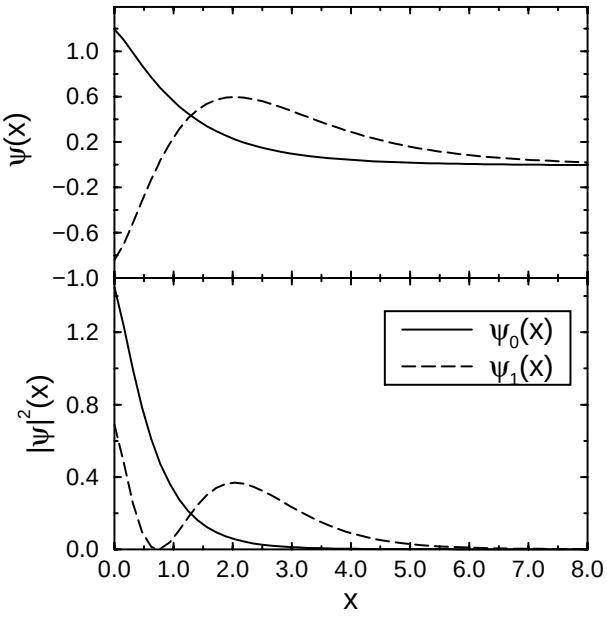

Fig. 5. Ground state and first excited state wave functions $\psi_0(x)$ and $\psi_1(x)$ using a square root potential $V(x) = \sqrt{x}$ and linear kinetic energy $H_{kin} = |k|$ plus border corrections (see Eq. (16)). The corresponding energies are $e_0 = 1.049$ and $e_1 = 2.040$.

From this equation one sees that the reference to the bulk limit yields only a finite offset.

Note that calculating $\langle H'_D \rangle$ with respect to the undimerized ground state yielding a potential $V(x) \propto \delta$ is in the spirit of degenerate first order perturbation theory. The effect of the perturbation, here dimerization, in the subspace of the unperturbed elementary excitations is considered. Even though these excitations are not really degenerate they are arbitrarily close in energy so that none of them can be discarded.

The calculation of $\langle H'_D \rangle$ is a perfect task for the DMRG approach [36,37], especially since we deal with open boundary conditions. The results are shown in Figure 4. We use the infinite system algorithm [37], keeping 100 states in each step. The error in the energies due to basis truncation is found to be smaller than 10^{-5}. One clearly observes a sublinear increase of $\langle H'_D \rangle$ with the chain length. Without frustration ($\alpha = 0$) a square root power law fits the data perfectly if a small offset on the x-axis is taken into account. For larger frustration larger exponents yield better fits. The inset, however, shows that for longer chain lengths ($L > 50$), the square root behavior is recovered for $\alpha \leq \alpha_c$ which can be seen from the linear behavior of the squared values. The frustration value $\alpha = 0.35$ is included to show that for this value relatively close to the critical one a linear behavior $\langle H'_D \rangle \propto L$ cannot yet be seen.

Another evidence that for $\alpha < \alpha_c$ the expectation value $\langle H'_D \rangle$ rises proportional to $\sqrt{L}$ stems from the dimension 1/2 of the dimerization operator [32]. By integration $\int^L dx/\sqrt{x} \propto \sqrt{L}$ follows the conjectured behaviour.

So our conjecture of a square root confining potential for lower frustrations is corroborated by direct calculations. We are now in the position to perform an analysis as in equations (21–25). Starting from the generalized Schrödinger equation with the border effect corrected kinetic part H'_{kin} (Eq. (16))

$$E\psi = v_S H_{kin}[\psi] + \delta A \sqrt{x}\psi \tag{27}$$

we rescale by $x = \xi y$ with

$$\xi = \left(\frac{v_S}{\delta A}\right)^{2/3} \tag{28}$$

where v_S is the spin wave velocity and A some constant which can be deduced from fits to data as in Figure 4. Equation (27) becomes

$$e_i \psi_i = H'_{kin}[\psi_i] + \sqrt{y}\psi_i \tag{29}$$

from which the energies are found using

$$E_i = e_i (\delta^2 A^2 v_S)^{1/3}. \tag{30}$$

The resulting two first wave functions are shown in Figure 5. The dimensionless energies are $e_0 = 1.049$

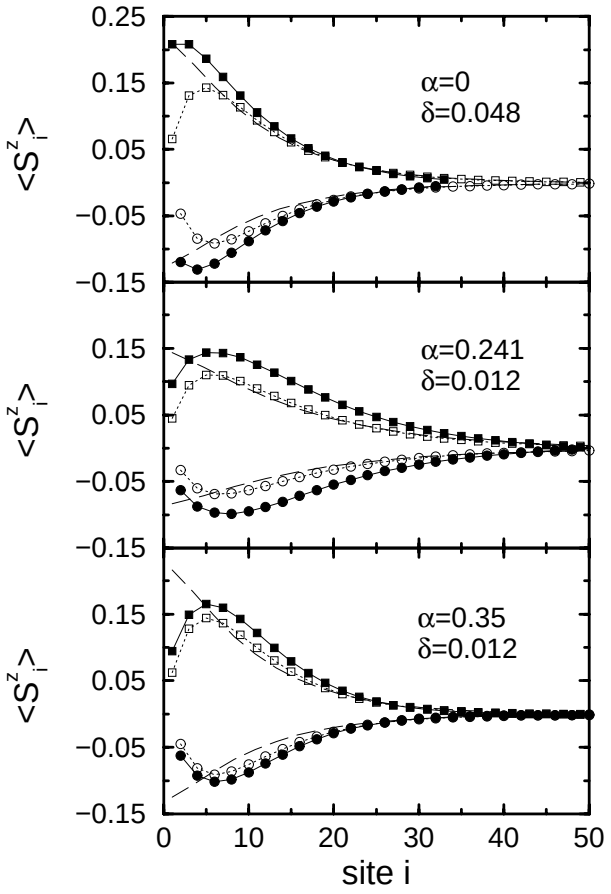

Fig. 6. Local magnetizations at dimerized chain ends with weak bonds for various values of α and δ. S^z_{tot} is set to 1/2. Squares: odd sites; circles: even sites; filled symbol: DMRG; open symbols: discrete bound spinon calculation; dashed lines continuous bound spinon calculation.

and $e_1 = 2.040$. Equation (29) is solved numerically by equidistant discretization and fast Fourier transform with up to 2^{19} points. Due to the singular behavior of equation (29) the precision is only of about 10^{-3}. But this is sufficient for the intuitive description that is being proposed here.

Note that due to the border correction (Eq. (16)) the wave functions do not vanish at the chain end, *i.e.* at $x = 0$. Furthermore, the wave functions decay rapidly as $x \to \infty$, but not following an exponential form, *e.g.*
[17,23], but rather a power law $\psi(x) \propto 1/x^3$. This is due to the highly non-local character of the kinetic energy (Eq. (14)). Thereby, we do not want to claim that the decay for large x follows indeed a power law. The picture we are presenting does not contain the generation of further spinon-antispinon pairs since it is a quantum mechanical, *single* particle scenario. It is the pair creation possible for energies larger than the gap Δ_{trip} which eventually leads to the exponential decay of the spinon probability. Our picture works best at intermediate distances as we will show in comparison to the DMRG data in the next section.

4 Results: Chain ends

Now we are in the position to compare results of bound spinon calculations directly against numerical results. The latter are obtained using the DMRG technique [36,37] for open boundary conditions with between $m = 24$ to 32 states kept in the iterations. The results are shown in Figure 6. Quantum mechanical bound spinon calculations are carried out in two ways. One is the continuum one relying on equations (6, 7, 16), the input for the spin wave velocity equation (13) and the potential parameters for a square root potential (see caption of Fig. 4). This means that one takes the result for $|\psi(x)|^2$ in Figure 5 and rescales $|\psi(x)|^2 \to |\psi(x/\xi)|^2/\xi$ with ξ from equation (28). The relevant values are $\xi = 16.1$, 23.5, and 15.6 for the uppermost to the lowermost panel in Figure 6. The results are shown as dashed curves.

The other one is a discrete treatment relying on equations (10, 12, 17). The results are depicted with open symbols. The values of the potential are those read off Figure 4 with $V(2i+1) = \langle H'_D(L = 2i)\rangle$. For simplicity the very good power law fits (dashed lines in Fig. 4) are used for the numerics.

The agreement between the DMRG results and the bound spinon model is very good, especially in view of the simplicity of the model. The shape of the curves are very well described by the bound spinon results. In particular, the correct binding length is predicted. This is in particular interesting since we know that the quantum mechanical model does not display an exponential decay. This means that the exponential tail matters only at larger lengths. For intermediate lengths, where the main weight is found, the bound spinon calculations work very well. The main feature that is included by the disrete calculation is the decrease of the amplitude for the first four to five sites. It results from the properties of equations (10, 12) and can thus be attributed to border effects which were neglected in equations (6, 7) but properly taken into account in equations (10, 12). It is *not* due to the dynamics of the problem. The very good agreement of the open-symbol curves and the long-dashed curves for larger distances underlines the applicability of the approximation (4).

The overall amplitude is larger than the one predicted by the bound spinon model. Since the basis we used included only the shortest range singlets it is not surprising that the true antiferromagnetic correlations are in fact larger. Thus we view the bound spinon results in this respect as a lower bound for the antiferromagnetic correlations. But it is interesting that even for the amplitudes the agreement is reasonable for correlation lengths ξ around 15. For larger values of ξ (middle panel in Fig. 6) the agreement becomes not as good.

Another point that can be addressed easily within the bound spinon model are excitation energies, namely the energy difference $E_1 - E_0$ (30) between the ground

state ψ_0 and the first excitetd state ψ_1, see Figure 5. The continuum (discrete) calculation yields 0.97 (0.10), 0.048 (0.055), and 0.061 (0.073) for the three cases in Figure 6 in descending order. It is not surprising that the continuum calculation provides lower values since it assumes a potential with smaller exponent, see Fig. 4), so that the distances between the energy levels become smaller. A smaller exponent implies that the potential increase for smaller arguments is larger than for larger arguments. Thus the smaller of two consecutive eigenenergies is lifted with respect to the larger one since the wave function belonging to the smaller eigenenergy is more localized. This effect explains also why the deviation is the largest for $\alpha = 0.35$ where the deviation of the optimum fit exponent to 1/2 is largest.

It was mentioned before that the occurrence of the triplet gap in dimerized systems can be viewed also as a binding phenomenon, see *e.g.* [11,13]. In this case, two spinons bind. However, since only the relative coordinate matters, this problem is almost equivalent to the binding of a single spinon to a chain end. The main difference is that the kinetic energy is doubled since both interaction partners move. So it is understandable that the ratio $(E_1 - E_0)/\Delta_{trip}$ is fairly constant. The triplet gaps Δ_{trip} as read off Figure 3 are 0.225, 0.116, and 0.162. The ratios of the continuum (discrete) values are 0.43 (0.46),0.42 (0.47), and 0.37 (0.45). Similar to the result found previously (0.6) [13] the transition from the ground state to the first excited one is at about half the triplet gap. This implies that it should be observable in scattering experiments as a rather sharp feature within the gap. Indeed, Raman scattering results have revealed such a feature in Zn-doped $CuGeO_3$ [13] even though the energy is higher than the one-dimensional model predicts.

It is clear that at energies $E_0 + \Delta_{trip}$ pair production becomes possible as it is known in QCD. The gedanken experiment of separating quarks in space in spite of the confinement results in the production of new quark pairs. In our situation any excited bound state can decay by producing a pair of spinons at low values of momentum if its energy fulfills $E_i \geq E_0 + \Delta_{trip}$. This mechanism gives rise to a continuum which sets in at $E_0 + \Delta_{trip}$. Thus higher energy bound states are no longer true eigenstates of the problem but have a finite lifetime since they might decay. The discrete calculation actually shows that E_4 and higher are no longer stable. This means that besides E_1, also E_2 and E_3 should exist as distinct sharp modes. Experimentally there is so far no indication for these higher modes. But it should be borne in mind that any deviation from pure $d = 1$ behavior tends to decrease the binding energies. Bound states are shifted closer to the continuum or even disappear in the continuum due to higher dimensional effects, see also [13,38].

In Figure 7 we show the same results as in Figure 6 but for the Majumdar-Ghosh point $\alpha = 0.5$. They are based on equations (21, 6, 7) in the continuum case. In the discrete case we used equations (20, 10, 12). The discrete kinetic energy used is nearest neighbor hopping such that the quadratic minimum is the same as for equation (21).

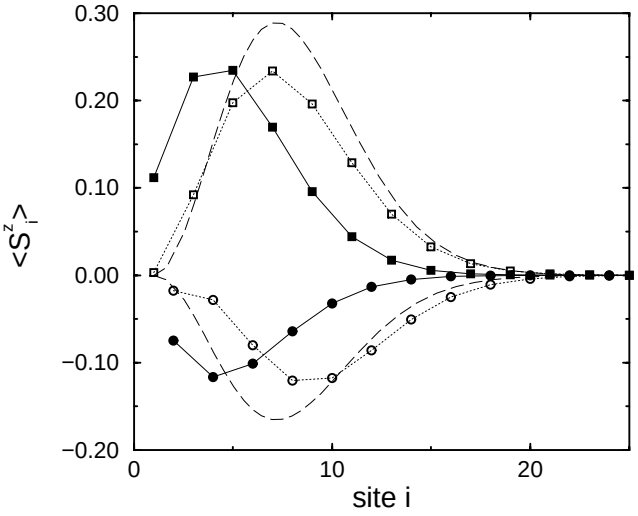

Fig. 7. Same as Figure 6 but for $\alpha = 0.5$ and $\delta = 0.012$.

One should expect an improved agreement since the kind of basis we are working with is particularly suited for the Majumdar-Ghosh point [15,16]. The agreement, however, is not very good. It becomes decisively better if the bound spinon results are shifted by about three lattice spacing. Probably dynamic border effects not taken into consideration by the basic assumptions concerning the kinetic and the potential energy (focused on the low energy behavior) are important. The binding length ξ for the Majumdar-Ghosh model according to equation (22) is only 4.7. Thus a low-energy approach might be insufficient for such a small binding length.

Interestingly, Eggert and Affleck found in a comparison of continuum field theoretical results with numerical data at $\delta = 0$ also that the agreement is much better if the continuum results are shifted by two sites towards the chain end [39]. An understanding of either of these observations would help to understand the other.

5 Results: Kink defects

Spin-Peierls systems are characterized by a coupling of magnetic (quasi) one-dimensional spin degrees of freedom to the lattice degrees of freedom, *i.e.* vibrating distortions (for reviews see [40,41]). At low temperature and zero magnetic field the system is in the gapped dimerized (D) phase where the coupling strength J_i of the spin chain alternates from site to site. As the magnetic field is increased the gap becomes smaller and at a critical field H_c the phase changes to an incommensurably modulated (I) phase. This I phase can be viewed as a soliton lattice where equally spaced tanh-like zeros of the distortions δ_i occur. In the vicinity of each zero of the distortion a spinon $S = 1/2$ is localized, see [42] and references therein.

In Figure 8 the soliton lattice is illustrated. These results are found from an adiabatic calculation where the distortions are treated statically. Most of the investigations of the I phase assume static distortions.

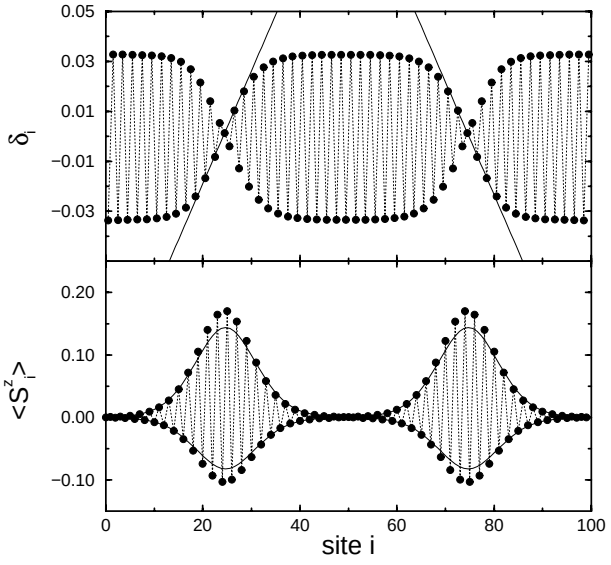

Fig. 8. Two solitons in a hundred site chain, *i.e.* $m = 1/100$, with periodic boundary conditions are studied (parameters $\alpha = 0.35$, $K = 8.7J$). In the upper panel, results from the self-consistent determined distortions δ_i (circles) which minimize $\langle H\rangle$ in (31) are shown. They are depicted between the sites since they belong to bonds. The straight lines are fits to the linear rising distortions with slope $s = 0.0045$. The lower panel displays the resulting local magnetizations (circles, DMRG calculation) and the bound spinon result (solid lines). For details see main text.

The Hamiltonian H from which Figure 8 is computed by minimization of the ground state energy with respect to $\{\delta_i\}$ reads [42]

$$H = H_{chain} + H_{Zeeman} + E_{elast} \tag{31a}$$

$$H_{chain} = \sum_{i=1}^{L} (J_i \boldsymbol{S}_i \cdot \boldsymbol{S}_{i+1} + J\alpha\, \boldsymbol{S}_i \cdot \boldsymbol{S}_{i+2}) \tag{31b}$$

$$H_{Zeeman} = -g\mu_B H S_z, \tag{31c}$$

$$E_{elast} = \frac{K}{2} \sum_i \delta_i^2, \tag{31d}$$

$$J_i = J(1 + \delta_i), \tag{31e}$$

where α denotes the relative frustration and S_z is the z component of the total spin of the L-site chain. The last two terms in equation (31) are the Zeeman energy and the elastic energy associated to the lattice distortion. A site independent spring constant K is used.

There are regions around site, *e.g.*, 50 where the distortion alternates as in the D phase. The corresponding local magnetization is essentially zero. Close to the linear zeros of the distortions at about sites 25 and 75 one observes a strongly alternating local magnetization which adds up to 1/2: $\sum_{i=0}^{50} \langle S_i^z\rangle = 1/2$. The distribution of local magnetizations is observable by NMR [43] and gives interesting information on the I phase and on the validity of the adiabatic treatment [44]. An interesting observation is that the ratio between the parallel magnetizations to the antiparallel magnetization at (roughly) the same sites is 7:4 as implied by equations (6, 7).

In this paper we are not interested in the self-consistent minimization of (31) but we take the $\{\delta_i\}$ as given and use the quantum mechanical picture developed above to show that the localized alternating magnetization in the vicinity of a zero of the distortion results from a bound spinon. The zero of the distortion is viewed as a kink defect. Since the δ_i on the odd (even) bonds change sign at the zero there is no simple short-range singlet pattern which ensures singlets at the stronger bonds without any free spin. Insofar the situation is comparable to the one at chain ends with weak bonds at the ends. The spinon bound to a kink defect is even simpler than the spinon bound to a chain end since no particular boundary effects on the kinetic energy need to be taken into account. Thus we use the continuum description based on equations (6, 7, 14).

The derivation of the attractive potential requires an additional assumption in order to treat also site dependent distortions. We find it natural to assume that the chain end potential $V(x)$ as determined from Figure 4 results from expectation values $\langle \mathbf{S}_i \cdot \mathbf{S}_{i+1}\rangle - \langle \mathbf{S}_i \cdot \mathbf{S}_{i+1}\rangle_{bulk}$ which decay like a power law with increasing distance from the ends

$$\begin{aligned} V(x) &= \delta a x^b \\ &= \frac{ab}{2} \int_0^x (\delta y^{b-1} + \delta (x-y)^{b-1}) dy, \end{aligned} \tag{32}$$

where we took into account that the chain end *and* the position of spinon constitute borders. The effect of these borders is treated approximatively as additive, *i.e.* as independent. A general power law with exponent b and prefactor a is dealt with. The advantage of equation (32) is that the distortion can be made site dependent $\delta \to \delta(x)$. In the vicinity of the kink defect, $\delta(x) = sx$ is a good description where s is an appropriately determined slope, see upper panel in Figure 8. A short calculation then leads to

$$\begin{aligned} V(x)_{kink} &= \frac{abs}{2} \int_0^{|x|} (y y^{b-1} + y(|x| - y)^{b-1}) dy \\ &= \frac{as}{2} |x|^{b+1}. \end{aligned} \tag{33}$$

Thus we obtain again a power law confining potential, the exponent of which is increased by one compared with the site-independent distortion. Moreover, the potential does not depend on whether the spinon moves to the right or to the left of the zero.

In Figure 9 a generic result for the localized state at a kink defect is shown. All parameters are set to unity. But rescaling permits, as before, to obtain the general relations

$$\xi = \left(\frac{2v_S}{as}\right)^{1/(2+b)} \tag{34a}$$

$$E_i = e_i \left(v_S^{1+b} \frac{as}{2}\right)^{1/(2+b)}. \tag{34b}$$

The solid lines in the lower panel in Figure 8 depict the convincingly good agreement between the bound spinon

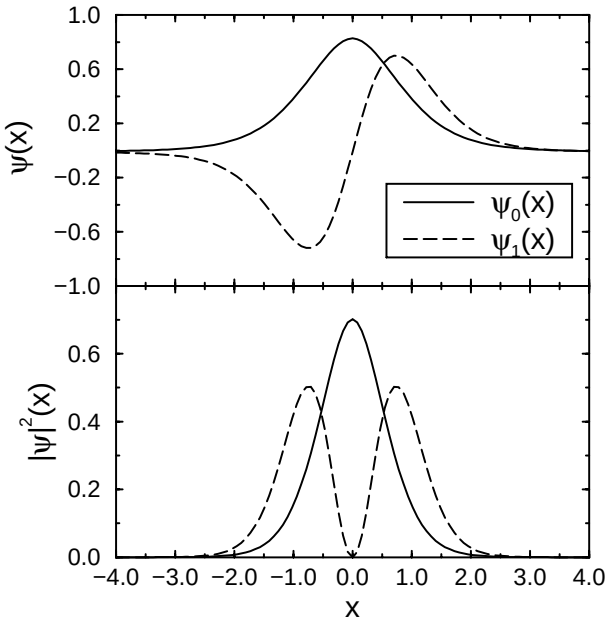

Fig. 9. Ground state and first excited state wave functions $\psi_0(x)$ and $\psi_1(x)$ using the integrated square root potential $V(x) = |x|^{3/2}$ and the linear kinetic energy $H_{kin} = |k|$ (see Eq. (14)). The corresponding energies are $e_0 = 1.051$ and $e_1 = 2.310$.

picture and the DMRG calculation. The value $s = 0.0045$ and the parameters of the dashed line fit to the $\alpha = 0.35$ data in Figure 4 is used for the binding length ξ in (34a).

6 Summary

In this work we have developed a quantum mechanical picture in the spirit of first order degenerate perturbation theory which describes the confinement of spinons due to dimerization. Without dimerization there is no confinement independently of the value of the frustration α. The picture works below and above the critical frustration of the undimerized chain $\alpha_c = 0.241$, even though the justification below α_c is less good. The main ingredients of the calculation are the known facts concerning the kinetic energy of the spinons which is linear below α_c and quadratic (plus a mass term) above α_c. From the dimer expectation values close to the borders of finite chains we deduced a potential $V(x)$ which is proportional to the dimerization δ. It was shown that this potential can be nicely fitted for intermediate distances ($L \approx 50$) by sublinear power laws below and just above $\alpha_c = 0.241$. For larger distances ($L \to \infty$) our results indicate that $V(x)$ increases like a square root for $\alpha \leq \alpha_c$ and linearly for $\alpha > \alpha_c$. To our knowledge, the fact that the confining potential below $\alpha_c = 0.241$ has to be sublinear has not been reported before in the literature.

The quantum mechanical picture describes very well the local magnetizations close to chain ends with weak bonds for intermediate ξ (≈ 20). A very good agreement is also found for the spinon bound to a kink defect. The sum of the moduli of the local magnetizations is (at least) enhanced by a factor 11/3 over the value for a single spin. For low ξ values the continuum description becomes less reliable. For large values of ξ the form of the site dependence of the local magnetization is still captured by our quantum mechanical picture. In particular, binding lengths can be easily estimated using equations (22, 28, 34a). The overall amplitude of the staggered component, however, is in fact larger for $\delta \to 0$ at $T = 0$ [39] .

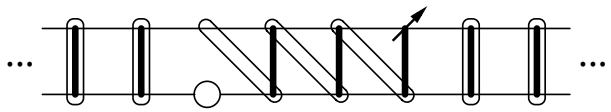

Fig. 10. Sketch of the singlet distribution on a doped ladder with strong bonds (thick solid lines) on the rungs. The open eyelets represent singlets. The circle indicates the defect (nonmagnetic dopant), the arrow the generated spinon after three hops. The misaligned diagonal singlets generate the confining potential.

Besides local magnetizations the eigenenergies of the bound states can be estimated easily within our approach. We find that in truly one-dimensional systems transitions to the first three excited states at chain ends should be possible. Any degree of higher dimensionality, however, will reduce this number.

The formation of gapful triplets can equally be viewed as binding of two spinons [11]. The essential differences to the case of chain ends are that the site variable denotes the relative coordinate between the spinons and that the kinetic energy is doubled since both interaction partners move.

The quantum mechanical picture is scale invariant. This means that for power law potentials the wave functions and energies can all be scaled to one universal case, see Figures 2, 5, and 9. Thus the quantum mechanical description provides a pedestrian approach to perturbations with anomalous dimensions and exponents. The anomalous exponents result naturally from the scaling behavior of the potential and the kinetic energy under changes of the length scale. A dimensional analysis implies already that for $V(r) = ar^b$ and $H_{kin} = c|k|^d$ the characteristic lengths scale like $\xi \propto (c/a)^{1/(b+d)}$ and the characteristic excitation energies like $E \propto (a^d c^b)^{1/(b+d)}$.

We like to point out that the basis states of our approach can be refined to take longer range antiferromagnetic correlations better into account. To this end longer range singlet pairs must be included and superposed. Dispersions and potentials can then be found by concepts similar to those proposed by Sutherland [45] for short range singlets in $d = 2$.

As an outlook to higher dimensions we present in Figure 10 the leading sketch of the singlet distribution on a ladder with strong bonds on the rungs. Ladders are objects of ample investigations. The alternating magnetizations [17,19,23] and enhanced antiferromagnetic correlations [21,22] indicate the similarity to open chains.

In Figure 10 the situation is depicted of the spinon (arrow) generated by the insertion of the defect (circle) after three hops on the upper leg. One clearly sees that the motion of such a spinon is also confined by a monotonic increasing potential. An increasing distance of the spinon from its original rung induces an increasing number of misplaced singlets. This leads to an increase in energy. From Figure 10 it is clear that the basic concepts of spinon motion and confining potential can be extended also to other RVB-type spin systems. The results discussed in this paper are not restricted to chains only.

We thank G. Els, P.H.M. van Loosdrecht, G. Martins, and E. Müller-Hartmann for helpful discussions. One of us (GSU) acknowledges the kind hospitality of the NHMFL, Tallahassee, where a large part of this work was carried out. We acknowledge financial support by the DFG through the SFB 341 and by the NSF grant DMR-9520776.

References

1. M. Hase, I. Terasaki, K. Uchinokura, Phys. Rev. Lett. **70**, 3651 (1993).
2. M. Isobe, Y. Ueda, J. Phys. Soc. Jpn **65**, 1178 (1996).
3. A.W. Garrett *et al.*, Phys. Rev. Lett. **79**, 745 (1997).
4. J.C. Bonner *et al.*, Phys. Rev. B **27**, 248 (1983).
5. B. Lake *et al.*, J. Phys.-Cond. **8**, 8613 (1996).
6. G. Chaboussant *et al.*, Phys. Rev. B **55**, 3046 (1997).
7. S. Liang, B. Douçot, P.W. Anderson, Phys. Rev. Lett. **61**, 365 (1988).
8. G.B. Martins, M. Laukamp, E. Dagotto, J.A. Riera, Phys. Rev. Lett. **78**, 3563 (1997).
9. T.-K. Ng, Phys. Rev. B **50**, 555 (1994).
10. D. Khomskii, W. Geertsma, M. Mostovoy, Czech. J. Phys. **46**, 3239 (1996).
11. I. Affleck, in *Dynamical Properties of Unconventional Magnetic Systems* (NATO ASI, Geilo, Norway, 1997).
12. G.B. Martins, E. Dagotto, J.A. Riera, Phys. Rev. B **54**, 16032 (1996).
13. G. Els *et al.*, Europhys. Lett. **43**, 463 (1998).
14. W.J. Caspers, K.M. Emmett, W. Magnus, J. Phys. A: Math. Gen. A **88**, 103 (1982).
15. E. Müller-Hartmann, G.S. Uhrig (in preparation).
16. B.S. Shastry, B. Sutherland, Phys. Rev. Lett. **47**, 964 (1981).
17. H. Fukuyama, T. Tanimoto, M. Saito, J. Phys. Soc. Jpn **65**, 1182 (1996).
18. M. Laukamp *et al.*, Phys. Rev. B **57**, 10755 (1998).
19. Y. Motome, N. Katoh, N. Furukawa, M. Imada, J. Phys. Soc. Jpn **65**, 1949 (1996).
20. H. Fukuyama, N. Nagaosa, M. Saito, T. Tanimoto, J. Phys. Soc. Jpn **65**, 2377 (1996).
21. M. Sigrist, A. Furusaki, J. Phys. Soc. Jpn **65**, 2385 (1996).
22. Y. Iino, M. Imada, J. Phys. Soc. Jpn **65**, 3728 (1996).
23. H.-J. Mikeska, U. Neugebauer, U. Schollwöck, Phys. Rev. B **55**, 2955 (1997).
24. M. Imada, Y. Iino, J. Phys. Soc. Jpn **66**, 568 (1997).
25. R. Jullien, F.D.M. Haldane, Bull. Am. Phys. Soc. **28**, 344 (1983).
26. K. Okamoto, K. Nomura, Phys. Lett. A **169**, 433 (1992).
27. R. Chitra *et al.*, Phys. Rev. B **52**, 6581 (1995).
28. H. Yokoyama, Y. Saiga, J. Phys. Soc. Jpn **66**, 3617 (1997).
29. J. des Cloizeaux, J.J. Pearson, Phys. Rev. **128**, 2131 (1962).
30. A. Fledderjohann, C. Gros, Europhys. Lett. **37**, 189 (1997).
31. M. Abramowitz, I.A. Stegun, *Handbook of Mathematical Functions* (Dover Publisher, New York, 1964).
32. M.C. Cross, D.S. Fisher, Phys. Rev. B **19**, 402 (1979).
33. G.S. Uhrig, H.J. Schulz, Phys. Rev. B **54**, R9624 (1996).
34. J.C. Talstra, S.P. Strong, P.W. Anderson, Phys. Rev. Lett. **74**, 5256 (1995).
35. J.C. Talstra, S.P. Strong, Phys. Rev. B **56**, 6094 (1997).
36. S.R. White, Phys. Rev. Lett. **69**, 2863 (1992).
37. S.R. White, Phys. Rev. B **48**, 10345 (1993).
38. G. Els *et al.*, Phys. Rev. Lett. **79**, 5138 (1997).
39. S. Eggert, I. Affleck, Phys. Rev. Lett. **75**, 934 (1995).
40. J.W. Bray, L.V. Interrante, I.C. Jacobs, J.C. Bonner, in *Extended Linear Chain Compounds*, edited by J.S. Miller (Plenum Press, New York, 1983), Vol. 3, p. 353.
41. J.P. Boucher, L.P. Regnault, J. Phys. I France **6**, 1939 (1996).
42. F. Schönfeld, G. Bouzerar, G.S. Uhrig, E. Müller-Hartmann, Eur. Phys. J. B **5**, 521 (1998).
43. Y. Fagot-Revurat *et al.*, Phys. Rev. Lett. **77**, 1861 (1996).
44. G.S. Uhrig, F. Schönfeld, J. Boucher, Europhys. Lett. **41**, 431 (1998).
45. B. Sutherland, Phys. Rev. B **37**, 3786 (1988).